npj | parkinson's disease

Article

Published in partnership with the Parkinson's Foundation

https://doi.org/10.1038/s41531-025-01087-9

Regulation of polyamine interconversion enzymes affects α-Synuclein levels and toxicity in a *Drosophila* model of Parkinson's Disease

Check for updates

Bedri Ranxhi[1], Zoya R. Bangash[1], Zachary M. Chbihi[1], Zaina Qadri[1], Nazin N. Islam[1], Sokol V. Todi[1,2], Peter A. LeWitt[1,2,3] ✉ & Wei-Ling Tsou[1] ✉

Parkinson's Disease (PD) is a neurodegenerative disorder characterized by α-synuclein accumulation and aggregation, leading to disrupted cellular homeostasis, impaired mitochondrial function, and neuroinflammation, ultimately causing neuronal death. Recent biomarker studies reveal elevated serum levels of L-ornithine-derived polyamines correlating with PD progression and clinical subtypes, though their precise role in PD pathology remains unclear. We investigated the impact of polyamine-interconversion enzymes (PAIEs) on α-synucleinopathy in a *Drosophila melanogaster* model of PD, evaluating key degenerative features such as lifespan, locomotor function, tissue integrity, and α-synuclein accumulation. Knockdown of ornithine decarboxylase 1 (ODC1), spermidine synthase (SRM), and spermine oxidase (SMOX) reduced α-synuclein toxicity, while suppression of spermidine/spermine N1-acetyltransferase 1 (SAT1) and spermine synthase (SMS) exacerbated it. Conversely, overexpressing SAT1 or SMOX significantly reduced α-synuclein toxicity, highlighting their potential role in PD. These findings underscore the critical role of polyamine pathways in modulating α-synuclein toxicity, offering novel therapeutic targets for PD.

Parkinson's Disease (PD) is a progressive neurodegenerative disorder affecting millions of mid-life individuals and is characterized by a decline in motor function (including slowed movements, tremors, and cognitive decline)[1,2]. The primary risk factor is increasing age, although environmental factors and genetics may also play a role[3–5]. The motor disorder of PD involves the degeneration of a specific population of neurons located in the substantia nigra, which project to the striatum and generate dopamine[6–8]. While most cases of PD appear sporadic[9], some cases arise from various gene mutations[5], the most common being *LRRK2*[10], *and GBA1*[11]. Additionally, more than two dozen gene mutations have been associated with causation or enhanced risk for PD[10,12]. While PD has multiple etiologies, a central hallmark of the disease is the pathological accumulation of α-synuclein (α-Syn)[13–15], a small, soluble protein encoded by the *SNCA* gene. α-Syn plays an essential role in synaptic function[16] and neurotransmitter release[17].

In PD, α-Syn undergoes structural changes, misfolding, and aggregation into insoluble fibrils[18]. These α-Syn aggregates, commonly seen in PD brain tissue in circular structures known as Lewy bodies[19], accumulate over time in the progressive disease and in aging individuals as an incidental finding[20]. Abnormal α-Syn aggregates interfere with critical cellular processes, including mitochondrial dynamics[21], proteostasis[22], and endo-lysosomal membrane integrity[23]. Ultimately, these processes result in selective neuronal damage and death. Thus, there is a need for mechanistic studies to further investigate disease-related α-Syn aggregation and its role in PD progression.

The aggregation process of α-Syn, driven by elevated α-Syn protein levels, is influenced by both genetic[4,24–29] and environmental factors[30–32]. Recent biomarker studies suggest that the concentration of polyamines (PAs) is altered in PD[33,34]. PAs are essential organic polycations that are evolutionarily conserved[35] across diverse organisms, from yeast and bacteria to plants and mammals. They are ubiquitous in cells and play critical roles in numerous cellular processes, including cell growth[36], nucleic acid synthesis[37,38], ion transport[37,38], and apoptosis[39,40]. Dysregulation of PA homeostasis can lead to various adverse outcomes[41] in

[1]Department of Pharmacology, Wayne State University School of Medicine, Detroit, MI, USA. [2]Department of Neurology, Wayne State University School of Medicine, Detroit, MI, USA. [3]Department of Neurology, Henry Ford Health Systems, Detroit, MI, USA.
✉e-mail: aa1142@wayne.edu; wtsou@wayne.edu

humans, culminating in disease and pathology; multiple reports link altered PA metabolism to various types of cancer[42–44], cardiovascular disease[45], and neurodegeneration[46–48]. Serum biomarker studies in PD identified an increase in three L-ornithine (ORN)-derived PAs, putrescine (PUT), spermidine (SPD), and spermine (SPM), in early-stage PD patients, all of which correlated with the progression of PD and its clinical subtypes[34]. Whether this correlation was related to the elevated α-Syn protein levels is unknown.

PAs can have a dual role in neurodegenerative diseases, functioning as facilitators that preserve neuronal integrity[49] by promoting autophagy to clear toxic proteins like α-Syn[50] and reduce oxidative stress, thus supporting neuronal survival. Conversely, PAs contribute to neuronal damage through their catabolism, which produces reactive oxygen species such as H_2O_2 and acrolein[51,52], leading to oxidative stress, inflammation, and excitotoxicity[53] that harm neurons[54]. The balance of PA pathways underscores their critical role in PD pathology[55,56]. However, it remains unclear whether elevated PA concentrations directly exacerbate PD pathology by promoting oxidative stress and inflammation, or if they are a secondary effect of disease progression, reflecting compensatory mechanisms to mitigate neuronal damage.

The intracellular homeostasis of ORN, PUT, SPD, and SPM is meticulously maintained through synthesis, degradation, and export[57,58]. PA biosynthesis converts ORN into PUT, and with further incorporation of aminopropyl groups into SPD and SPM through specific polyamine interconversion enzymes (PAIEs)[35]. These include PA anabolic and catabolic enzymes[59]. PA anabolic enzymes, such as ornithine decarboxylase (ODC1), spermidine synthase (SRM), and spermine synthase (SMS), facilitate the biosynthesis of PAs[57,58]. This process involves a series of decarboxylation reactions followed by aminopropylation[60]. PA catabolism is a more complex process in which PAs are broken down into their precursors and is facilitated by a distinct group of PAIEs that include spermine oxidase (SMOX), spermidine/spermine N^1-acetyltransferase (SAT1), and N^1-acetylpolyamine oxidase (PAOX)[61]. Catabolic PAIEs are involved in acetylation and oxidation processes[62,63]. Additionally, selective transporters mediate the translocation of PAs and their byproducts across cellular membranes. The Na^+-independent transporter SLC7A2[64] supports PA synthesis by facilitating the uptake of cationic amino acids and ORN. Furthermore, ATP-dependent transporters ATP13A2 and ATP13A3[65] are essential for PA trafficking within the endo-/lysosomal system, ensuring efficient distribution and homeostasis of PAs in cellular compartments. These mechanisms highlight the complex regulation of PA dynamics in cells. Investigating PA pathways—including metabolites, interconversion enzymes, and transporters[66,67]—may provide a better understanding of PD's pathogenic mechanisms, as indicated by the serum biomarker[33,34] and related findings[55].

Here, we utilized *Drosophila melanogaster* to investigate the significance of PA pathway perturbation in PD pathology, modeled through the neuronal overexpression of human wild-type α-Syn[68,69]. Our aim was to determine whether targeted PA metabolism could affect α-Syn stability and impact disease progression. We observed that the regulation of PAIEs significantly affects α-Syn toxicity. We identified the PA catabolic enzymes SAT1 and SMOX as critical factors in PD, as they influenced α-Syn protein levels and its effects in *Drosophila*. Our findings provide novel mechanistic insights into a PD model, using α-Syn pathology as a readout to advance biomarker research and set the stage for PA-targeted therapies.

Results

Expression of human α-Syn leads to shortened lifespan and motor dysfunction in *Drosophila*

We employed overexpression of human wild-type α-Syn as a *Drosophila* model to investigate the impact of PA pathway modulation in PD. As an initial step, we validated the model by assessing whether α-Syn expression induces neurodegenerative phenotypes when driven ubiquitously or specifically in neurons. As shown in Fig. 1A, ubiquitous expression of α-Syn using the sqh-Gal4 driver[70–72] resulted in a dose-dependent reduction in lifespan in both male and female flies, with two copies of the transgene reducing median lifespan to 64 days in females and 53 days in males. A more pronounced effect was observed with pan-neuronal expression of α-Syn driven by elav-Gal4, as illustrated in Fig. 1B. Flies carrying two copies of α-Syn had a median lifespan of 29 days in females and 18 days in males, compared to 76 days in females and 64 days in males with only one copy. These results confirm that α-Syn dosage strongly influences survival, particularly when expressed in neurons. Next, we examined a secondary aspect of fly physiology by assessing fly mobility through the Rapid Iterative Negative Geotaxis (RING) assay[73] (Fig. 1C). In this assay, fly positions across zones 1–5 indicate graded motor performance. Flies in zone 1 exhibit severe motor deficits, while those in zones 4 and 5 demonstrate strong climbing ability and preserved neuromuscular function. This distribution enables quantification of locomotor impairments and improvements following genetic interventions. The assay was conducted three and six weeks post-eclosion of flies ubiquitously expressing α-Syn (Fig. 1D). At week three, compared to control flies that contained the Gal4 driver in the absence of α-Syn, a smaller proportion of α-Syn-expressing flies reached zones 4 and 5, the highest tiers of the motility index. This decline in motility was also dose-dependent, with flies carrying two copies of the α-Syn transgene exhibiting a more pronounced impairment in both sexes. Notably, sex-specific differences emerged at week six, with a higher proportion of male flies expressing one or two copies of α-Syn remaining in zone 1 compared to their female counterparts, indicating more severe locomotor deficits. These sex-specific differences mirror observations in human populations, where PD is more common in men, with ~65% of patients being male[74,75].

We also conducted the same RING assay on flies overexpressing α-Syn pan-neuronally (Fig. 1E). Due to the early mortality observed in flies with pan-neuronal α-Syn expression, we performed assays at 3 and 4 weeks post-eclosion. Pan-neuronal expression of α-Syn led to markedly greater locomotor impairments compared to flies with ubiquitous α-Syn expression. Notably, at both 2 and 4 weeks, 96–100% of male flies carrying two copies of the α-Syn transgene remained confined to zone 1 at the bottom of the vial, highlighting the severity of the phenotype. Sex-specific differences were observed as early as week two in flies pan-neuronally expressing two copies of the α-Syn transgene, with the proportion of males remaining in zone 1 being ~30% higher compared to females. We conclude that expression of α-Syn in flies leads to reduced motility and longevity in a dose-dependent manner. These baseline data establish the α-Syn overexpression fly model as a valuable tool for investigating the relationship between PA metabolism and α-Syn toxicity.

Targeting of PAIE modulates α-Syn toxicity in *Drosophila*

Given the elevated levels of PAs observed in the serum of PD patients[33,34], we sought to determine whether regulating the PA pathway could influence disease-related phenotypes in our PD model. To address this, we examined the effects of PA pathway modulation in our *Drosophila* model with pan-neuronal expression of α-Syn. As illustrated in Fig. 2A, the PA pathway constitutes a tightly regulated metabolic network comprising anabolic and catabolic interconversion enzymes, along with transporters that collectively maintain PA homeostasis. To assess how individual PAIEs influence α-Syn-driven neurodegeneration, we performed RNAi-mediated neuronal knockdowns of *Drosophila* orthologs of PAIEs and PA transporters. The efficiency of each gene knockdown was validated by quantifying PAIE mRNA levels in the presence and absence of RNAi-mediated knockdown using qRT-PCR (Supplementary Fig. 1).

In our longevity assays, knockdown of ODC1 (Fig. 2B, J), SRM (Fig. 2C, K), or SMOX (Fig. 2G, O) significantly extended lifespan in both female and male α-Syn flies compared to RNAi controls. Notably, knockdown of SAT1 reduced lifespan in female flies (Fig. 2F) but not in males (Fig. 2N), suggesting a sex-specific effect. Additionally, neuronal knockdown of PAOX, ATP13A3, or SLC7A2, regardless of α-Syn expression, led to pronounced developmental abnormalities such as unexpanded wings and impaired leg mobility, resulting in early lethality (Fig. 2E, H, I, M, P, Q). These findings indicate that these genes are essential for normal development and function

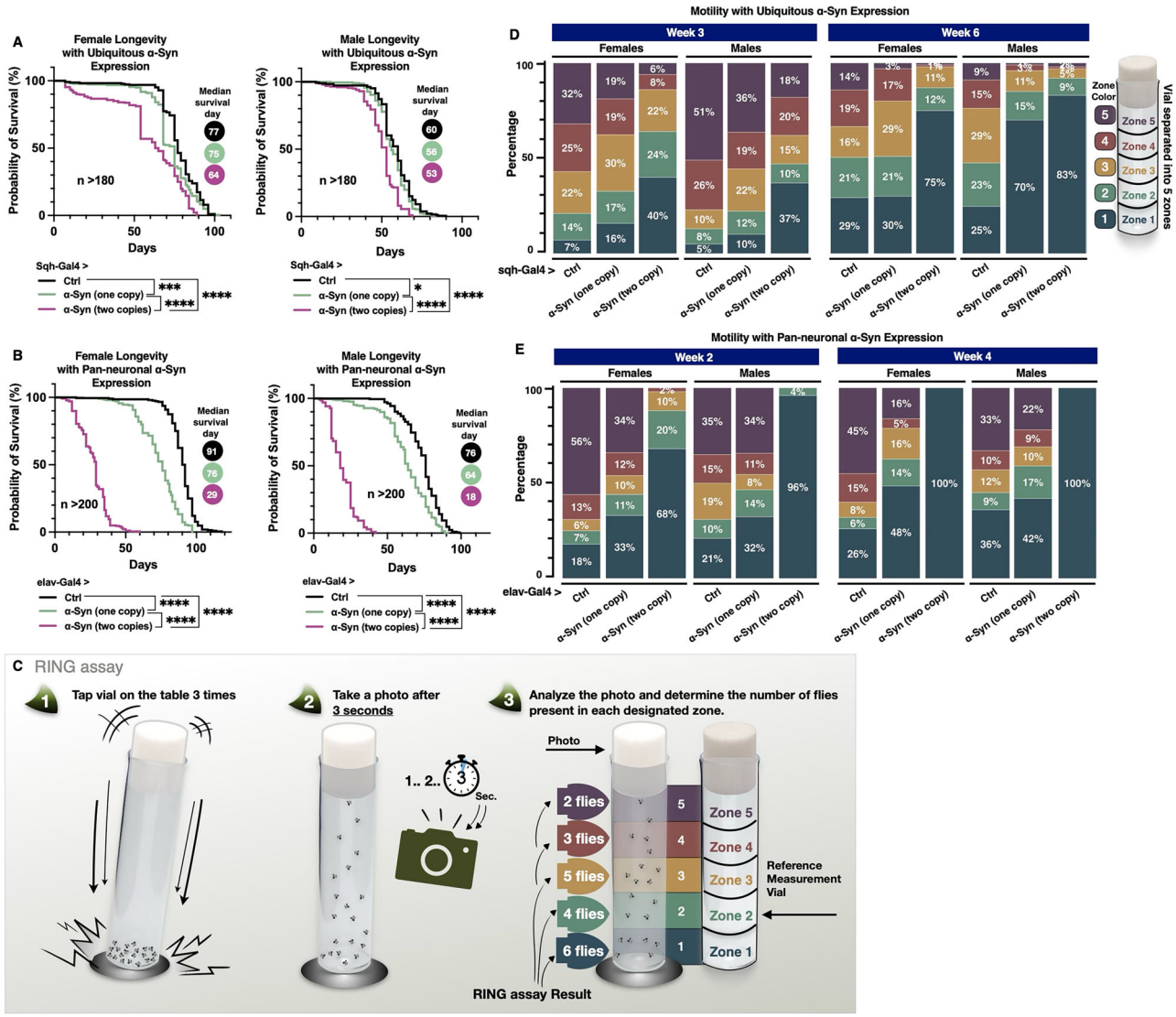

Fig. 1 | Longevity and motility analyses of flies ubiquitously or pan-neuronally expressing α-Syn. A, **B** Longevity curves of adult female (left) and male (right) flies expressing zero (black), one (green), or two (pink) copies of α-Syn throughout development and adulthood, driven by (**A**) sqh-Gal4 and (**B**) elav-Gal4. Median survival days are indicated to the right of each panel. Statistical significance was assessed using log-rank tests: ns (not significant), *($p < 0.05$), **($p < 0.01$), ***($p < 0.001$), ****($p < 0.0001$). **C** Diagram illustrating methodology of the Rapid Iterative Negative Geotaxis (RING) assay. For details, please see the Methods section. **D**, **E** Motility analysis (RING assay) of flies with (**D**) ubiquitous and (**E**) pan-neuronal α-Syn expression, with the week of measurement indicated at the top. Each vial was divided into five zones, with different colors representing each zone. Flies were photographed, and the number of flies in each zone was counted and normalized to the total number of flies. The percentage of flies in each zone is shown in the figure.

independently of α-Syn-associated toxicity. Due to these developmental defects, proper lifespan comparisons under α-Syn expression could not be assessed for these knockdowns. In summary, the lifespan extension observed following ODC1, SRM, or SMOX knockdown highlights the potential protective role of modulating specific PAIE pathways in the context of α-Syn-induced pathology.

Next, we examined whether modulation of PAIEs affects the motility of the α-Syn *Drosophila* model using the RING assay (Fig. 3). In week one, knockdown of SMS and SAT1 impaired climbing ability in female flies, with fewer individuals reaching the higher zones (4 and 5); notably, SAT1 knockdown led to a statistically significant reduction in the percentage of flies in zones 4 and 5 ($p = 0.0027$), and 50% of flies remaining in zone 1 (Fig. 3A). In male flies, knockdown of ODC1, SRM, SMOX, or SAT1 initially enhanced climbing performance (Fig. 3B), with a greater proportion reaching zone 5 and fewer remaining in zone 1. ODC1 knockdown resulted in a statistically significant improvement in climbing ability ($p = 0.0351$). As observed in the longevity experiments (Fig. 2), knockdown of PAOX, ATP13A2, or SLC7A2 caused severe developmental abnormalities. These flies displayed a complete inability to climb and remained in zone 1 at the bottom of the vial (Fig. 3A, B).

By the fourth week, female flies with knockdown of SRM or SMOX showed a marked improvement in mobility, as indicated by a higher proportion of flies reaching zone 5 and fewer remaining in zone 1 (Fig. 3C). For SMOX knockdown, the combined percentage of flies in zones 4 and 5 was significantly increased ($p < 0.0001$). In contrast, knockdown of ODC1, SMS, or SAT1 resulted in reduced mobility, with fewer females reaching zone 5. In males, knockdown of ODC1, SRM, or SMOX (Fig. 3D) enhanced locomotor performance, with a greater percentage of flies reaching zone 5 compared to controls. Conversely, knockdown of SMS or SAT1 led to decreased motility, with fewer flies reaching zone 5 and more remaining in zone 1. By the eighth week, SMOX knockdown continued to promote improved motor function, with 33% of both female (Fig. 3E) and male (Fig. 3F) flies reaching zone 5, compared to only 12% and 8% in the respective control groups. The combined proportion of flies in zones 4 and

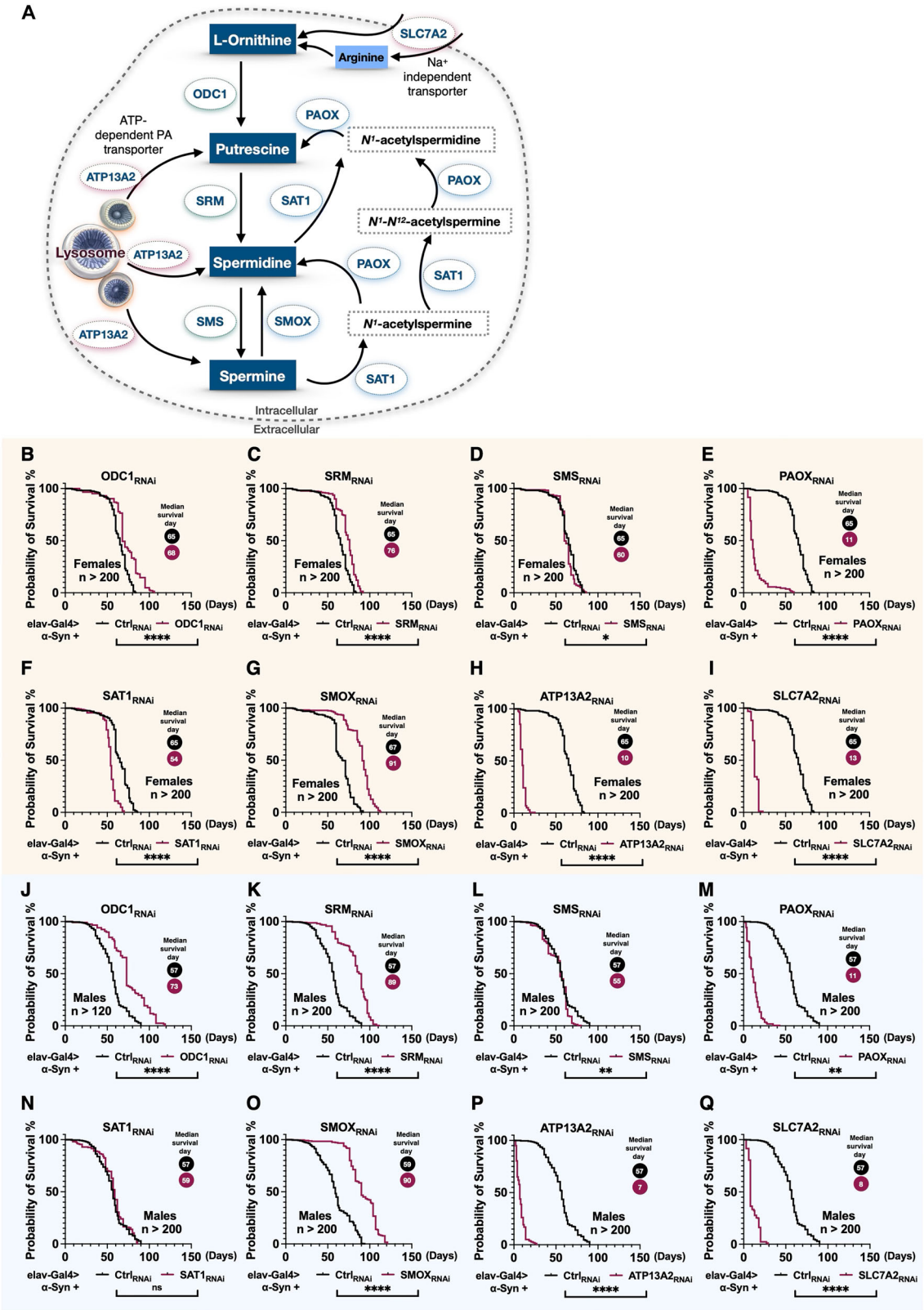

Fig. 2 | Knockdown of enzymes in the polyamine pathway alters longevity in the α-Syn *Drosophila* model. A Schematic of the polyamine pathway and the associated enzymes. **B**–**Q** Longevity analysis of neuronal knockdown of individual polyamine pathway enzymes in the α-Syn *Drosophila* model. **B**–**I** Show lifespan data for female flies, while panels (**J**–**Q**) present data for male flies. Statistical significance was determined using log-rank tests: ns (not significant), *($p < 0.05$), **($p < 0.01$), ***($p < 0.001$), ****($p < 0.0001$).

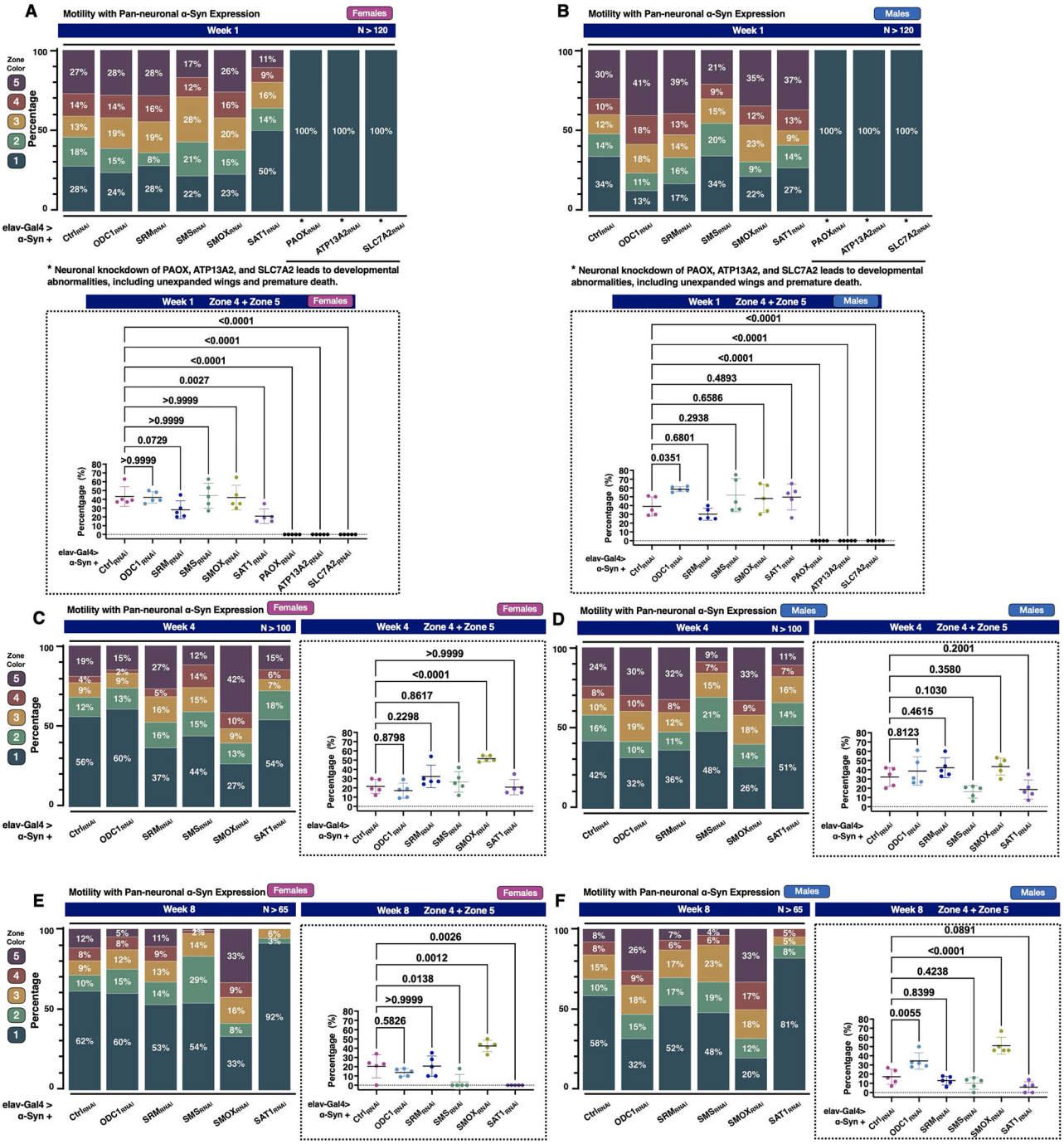

Fig. 3 | Knockdown of enzymes in the polyamine pathway impacts motility in the α-Syn *Drosophila* model. A–F RING assay results showing the effects of neuronal knockdown of individual polyamine pathway enzymes in the α-Syn *Drosophila* model at week 1 (**A**, **B**), week 4 (**C**, **D**), and week 8 (**E**, **F**), with female flies on the left and male flies on the right. In (**A**, **B**), asterisks indicate that flies with neuronal knockdown of PAOX, ATP13A2, and SLC7A2 were assessed only at week 1, as these flies exhibited severe developmental abnormalities, including unexpanded wings, and died within three weeks. Higher zone-specific comparisons from each RING assay are shown in (**A**, **B**), and on the right side of (**C**–**F**). The total percentage of flies in Zones 4 and 5 was calculated for each vial, with each group consisting of five vials containing 20 flies per vial. Statistical analysis was performed using one-way ANOVA followed by Dunnett's multiple comparisons test against the $Ctrl_{RNAi}$ group, using GraphPad Prism.

5 was significantly increased in both sexes (female: $p = 0.0012$; male: $p < 0.0001$). Interestingly, ODC1 knockdown led to improved mobility exclusively in males (Fig. 3F), with 26% reaching zone 5 and 32% remaining in zone 1. A significantly greater proportion of flies occupied zones 4 and 5 ($p = 0.0055$). Knockdown of SAT1 consistently impaired locomotor function in both sexes, with most flies confined to zone 1 (92% in females and 81% in males). Knockdown of SMS also reduced motility, though to a lesser extent, with only 1% of females and 4% of males reaching zone 5. Together, these findings indicate that SMOX knockdown significantly improves locomotor outcomes in the α-Syn model, while SAT1 knockdown consistently worsens them.

PAIE regulates fly eye integrity in the context of α-Syn-induced toxicity

We observed that neuronal PAIE knockdown influences longevity and motility phenotypes in the α-Syn model. To investigate whether these effects

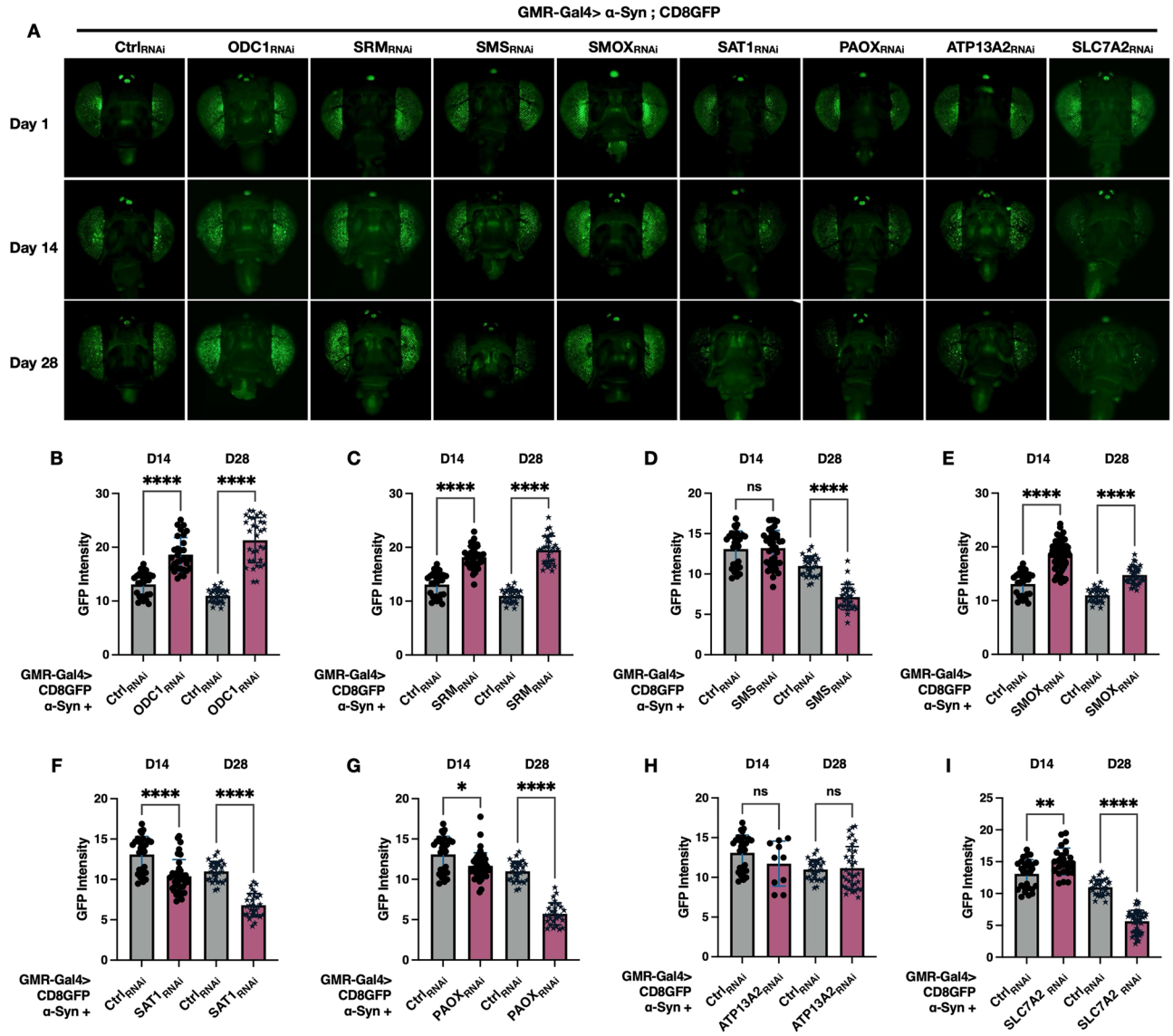

Fig. 4 | Polyamine pathway enzyme knockdown modulates eye integrity in the α-Syn *Drosophila* model, assessed by CD8GFP fluorescence. A Representative GFP images of fly heads co-expressing CD8GFP, α-Syn, and RNAi targeting polyamine pathway enzymes in the eye. Female fly head images were gathered on days 1, 14, and 28 post-eclosion. **B**–**I** Quantification of GFP fluorescence intensity at days 14 and 28 using ImageJ. Sample size: $N \geq 15$ per condition. Statistical analysis was performed using Brown-Forsythe and Welch ANOVA tests. Significance levels: ns (not significant), *($p < 0.05$), **($p < 0.01$), ***($p < 0.001$), ****($p < 0.0001$).

are associated with cellular-level changes in neuronal integrity, we utilized the *Drosophila* eye, a well-established system for studying neurodegeneration and cellular toxicity. Each ommatidium of the compound eye contains a cluster of photoreceptor neurons. By expressing a membrane-tagged fluorescent marker, CD8GFP, in these photoreceptors, we were able to visualize cellular architecture and assess neuronal integrity in vivo[76–78]. This model provides a robust and quantifiable platform for evaluating α-Syn-induced toxicity in response to PAIE modulation. In this context, toxicity is reflected by the degeneration of internal ommatidial components, leading to photoreceptor cell loss and reduced GFP fluorescence[78]. Conversely, enhanced fluorescence indicates preserved eye structure and improved neuronal integrity[79]. Figure 4A represents the GFP photos of the female fly eyes, Showing a significantly enhanced GFP signal in the eyes of $ODC1_{RNAi}$, SRM_{RNAi}, and $SMOX_{RNAi}$ at days 1, 14, and 28. Quantification of GFP intensity (Fig. 4B-I) confirmed that knockdowns of ODC1 (Fig. 4B), SRM (Fig. 4C), or SMOX (Fig. 4E) at days 14 and 28 led to a notable increase in fluorescence compared to background controls. In contrast, flies co-expressing α-Syn with either $SAT1_{RNAi}$ (Fig. 4F) or $PAOX_{RNAi}$ (Fig. 4G) at days 14, and 28, as well as those with SMS_{RNAi} (Fig. 4D) at day 28, exhibited significantly reduced GFP intensity compared to the controls. Moreover, while knockdown of PA transport enzyme ATP13A2 did not alter GFP fluorescence (Fig. 4H), knockdown of the sodium-independent transporter SLC7A2 led to a significant GFP reduction at day 28 (Fig. 4I). Overall, these results indicate that knockdown of ODC1, SRM, and SMOX enhances cellular integrity in the α-Syn model, whereas knockdown of SAT1, SMS, PAOX, or SLC7A2 exacerbates cellular toxicity.

We conducted similar analyses in male fly eyes (supplementary fig. 2). Our results show that the overall patterns of neuronal integrity are largely consistent between males and females. Specifically, knockdown of ODC1, SRM, and SMOX increased neuronal integrity, while knockdown of SAT1, PAOX, and SLC7A2 reduced integrity in both sexes. The one notable exception is SMS knockdown at day 28: females exhibited a significant reduction in neuronal integrity compared to controls, while males did not. We believe this discrepancy is due to control males already exhibiting substantial neuronal degeneration by day 28, limiting the ability to detect further decline. In contrast, control females retained higher neuronal integrity at the same time point, allowing the effect of SMS knockdown to be more clearly observed. Collectively, these findings

underscore the significance of PAIE modulation in mitigating α-Syn-induced toxicity.

PAIE knockdowns affect α-Syn protein levels

To further understand how PAIE modulation influences α-Syn-induced toxicity, we next examined whether changes in PAIE expression affect α-Syn protein levels. Since α-Syn accumulation and aggregation are central features of PD pathology, we assessed α-Syn protein abundance in flies with pan-neuronal expression of α-Syn and RNAi-mediated knockdown of individual PAIE genes (Fig. 5A–H with quantification on the right). We observed significant increases in α-Syn protein levels following knockdown of SMS (Fig. 5C), ATP13A2 (Fig. 5D), and SAT1 (Fig. 5F). In contrast, α-Syn protein levels were reduced when PAOX (Fig. 5E) or SMOX (Fig. 5G) was knocked down. Knockdown of ODC1 (Fig. 5A), SRM (Fig. 5B), or SLC7A2 (Fig. 5H) did not result in notable changes in α-Syn levels. Together, these findings suggest that individual PAIE enzymes differentially regulate α-Syn protein homeostasis, with knockdown of PAOX and SMOX reducing α-Syn accumulation, while the knockdowns of SMS, SAT1, or ATP13A2 promote it.

Overexpression of SAT1 and SMOX mitigates α-Syn-induced toxicity in *Drosophila*

We have compared longevity, motility, eye integrity, and α-Syn protein levels in the α-Syn *Drosophila* models and discovered that suppressing enzymes in the PA pathway affects α-Syn-mediated toxicity. Given the strong effects we observed with $SAT1_{RNAi}$ and $SMOX_{RNAi}$, we were interested in whether overexpressing these genes would produce the opposite outcome and further support their regulatory roles. We generated new fly lines carrying UAS-DmSAT1 or UAS-DmSMOX by inserting *Drosophila* SAT1 or SMOX cDNA into the attP2 site on chromosome 3 (Fig. 6A–C). We utilized flies with pan-neuronal expression of two copies of α-Syn to induce a stronger phenotype and tested whether overexpression of DmSAT1 could rescue it. As expected, DmSAT1 overexpression significantly extended lifespan compared to control flies (Fig. 6D). Furthermore, DmSAT1 markedly improved climbing ability (Fig. 6E), with females showing a more pronounced enhancement than males, as significantly more flies reached the higher zones 4 and 5 (Fig. 6F). Western blot analyses also revealed a reduction in α-Syn protein levels in the presence of DmSAT1 overexpression (Fig. 6G).

Similarly, we tested flies with pan-neuronal expression of both DmSMOX and α-Syn. Intriguingly, despite the protective effects previously observed with SMOX knockdown, overexpression of DmSMOX also significantly extended the lifespan of α-Syn-expressing flies (Fig. 6H). RING assays showed improved climbing ability in both sexes, with males displaying a greater enhancement, as more flies reached zones 4 and 5 compared to females (Fig. 6I). Quantification of flies in zone 1 and zone 5 (Fig. 6J) further supports these findings. In females, SMOX overexpression significantly decreased the percentage of flies in zone 1 and increased those in zone 5. A similar trend was observed in males, with a significant reduction in zone 1 and an increase in zone 5. These results confirm that SMOX overexpression enhances motor performance in both sexes, with a more pronounced effect in males. Western blot analysis further confirmed that SMOX overexpression significantly reduced α-Syn protein levels (Fig. 6K). This dual outcome, in which both suppression and overexpression of SMOX attenuate α-Syn toxicity, was unexpected and suggests a more nuanced role for SMOX in regulating PA metabolism and α-Syn homeostasis. Collectively, these findings support the conclusion that overexpression of either SAT1 or SMOX mitigates α-Syn toxicity in *Drosophila* models.

Discussion

In this study, we systematically investigated the role of PA pathway enzymes in modulating α-Syn-induced toxicity using an intact organism model. Previous reports of elevated L-ORN-derived PAs in the serum of PD patients[34] suggest a potential systemic disruption in PA metabolism. Given the tightly regulated nature of PA homeostasis[80], we hypothesized that altered concentrations of the various PAs contribute to PD pathology, as proposed in prior studies[55,81]. To test this, we examined the functional relevance of the PA pathway in a *Drosophila* model of α-Syn toxicity, with a particular focus on PAIEs and PA transporters. Our findings demonstrate distinct phenotypic outcomes associated with specific gene knockdowns, highlighting the importance of PA metabolism in synucleinopathy and its potential as a therapeutic target (Fig. 7).

The modulation of α-Syn protein levels by PAIEs observed in our Western blot analyses (Figs. 5 and 6) suggests that these enzymes regulate α-Syn through multiple mechanisms. Several PAIEs likely influence protein turnover via the ubiquitin-proteasome system or autophagy. For instance, SMOX activity generates reactive oxygen species, which can alter autophagic flux or induce oxidative modifications that affect α-Syn aggregation and clearance[82,83]. SAT1, known for its role in PA catabolism and acetylation pathways, may influence α-Syn stability by affecting lysosomal degradation or proteasomal activity[50,84,85]. Moreover, PAs such as spermidine are essential for eIF5A hypusination[86,87], a process that modulates translation elongation and may indirectly influence the production or handling of α-Syn and other proteostasis-related proteins[88]. Although transcriptional regulation seems less likely, post-transcriptional mechanisms, including mRNA stability and translation efficiency, may also contribute to the observed changes. Future studies will need to differentiate among these and other possibilities.

The α-Syn toxicity readouts in knockdown experiments, including longevity, motility, and GFP eye integrity assays, closely correlate with α-Syn protein levels. This highlights the functional impact of PA pathway modulation on α-Syn homeostasis and associated neurodegenerative phenotypes (Fig. 7). Among the enzymes tested, SAT1 showed the most pronounced effect. Knockdown of SAT1 exacerbated α-Syn toxicity, resulting in elevated α-Syn protein levels, increased structural degeneration in the fly eye, reduced lifespan, and impaired motility. In contrast, SMOX knockdown produced the opposite outcome, lowering α-Syn protein levels, improving eye integrity, extending lifespan, and enhancing motor performance. Notably, both SAT1 and SMOX are catabolic enzymes in the PA pathway, raising an important question: why does knockdown of each result in such divergent effects? Further investigation is needed to examine the roles of specific metabolic byproducts and the balance of individual PA species in shaping these outcomes. Suppression of ODC1 and SRM improved longevity and eye integrity, while motility was enhanced in ODC1 knockdown males and SRM knockdown flies before week 4; however, α-Syn protein levels remained unchanged. Knockdown of SMS resulted in increased α-Syn levels, yet only worsened motility and eye integrity, with no significant effect on lifespan. These findings suggest that distinct PAIEs differentially regulate α-Syn toxicity, either directly or indirectly; they highlight the complex role of PAIEs in α-Syn-associated neurodegeneration.

We observed sex-specific differences in survival motor function across nearly all conditions in the α-Syn *Drosophila* model. As shown in Fig. 2, female flies exhibited longer median lifespans than males in both control and PAIE knockdown groups. This female-biased longevity is consistent with prior findings in *Drosophila* and other model organisms, where females often demonstrate greater resilience to neurodegenerative insults[75,89,90]. Although the precise mechanisms underlying this sex disparity remain unclear, several biological factors may contribute. In *Drosophila*, females are generally larger than males and tend to possess stronger wings and legs[91], which may enhance their physiological robustness. These physical traits are likely governed by intrinsic, sex-specific gene regulatory networks. Additional contributing factors may include differences in mitochondrial function, redox homeostasis, hormonal signaling, and immune response pathways[75]. This observation has potential relevance to human disease, as approximately 65% of PD patients are male[74,92,93], a sex disparity for which the underlying biological basis remains unresolved. Our findings underscore the importance of incorporating sex as a biological variable in neurodegeneration research and suggest that identifying protective mechanisms in females could reveal novel therapeutic targets.

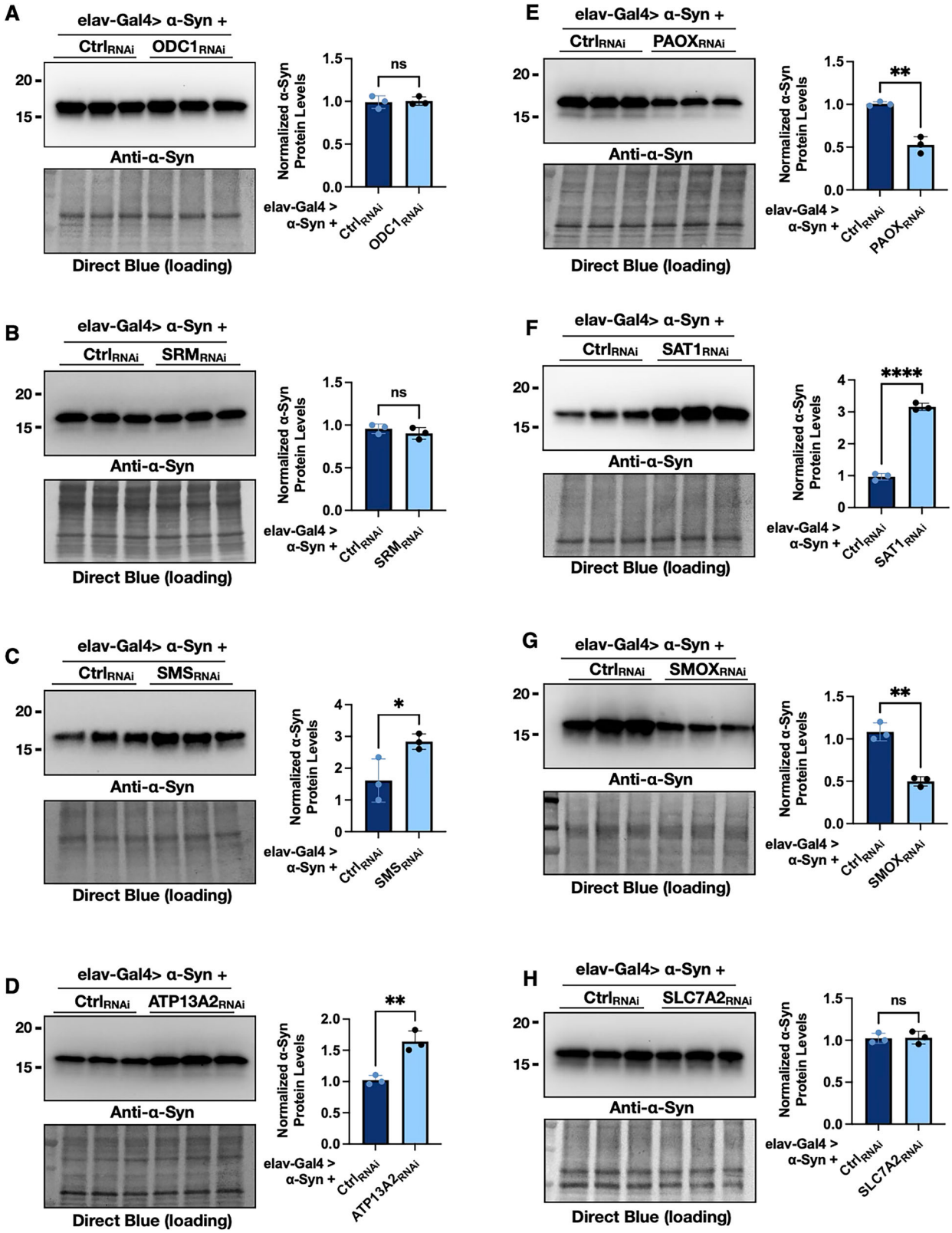

Fig. 5 | Polyamine pathway enzyme knockdown modulates α-Syn protein levels. **A**–**H** Western blot analyses of α-Syn protein levels in flies with pan-neuronal expression of α-Syn following RNAi-mediated knockdown of specific polyamine pathway enzymes. Normalized α-Syn protein levels were calculated by normalizing the intensity of the α-Syn bands to the corresponding total protein signal from Direct Blue. Statistical significance was assessed using an unpaired two-tailed Student's *t* test. Significance levels are indicated as follows: ns (not significant), *($p < 0.05$), **($p < 0.01$), ***($p < 0.001$), ****($p < 0.0001$).

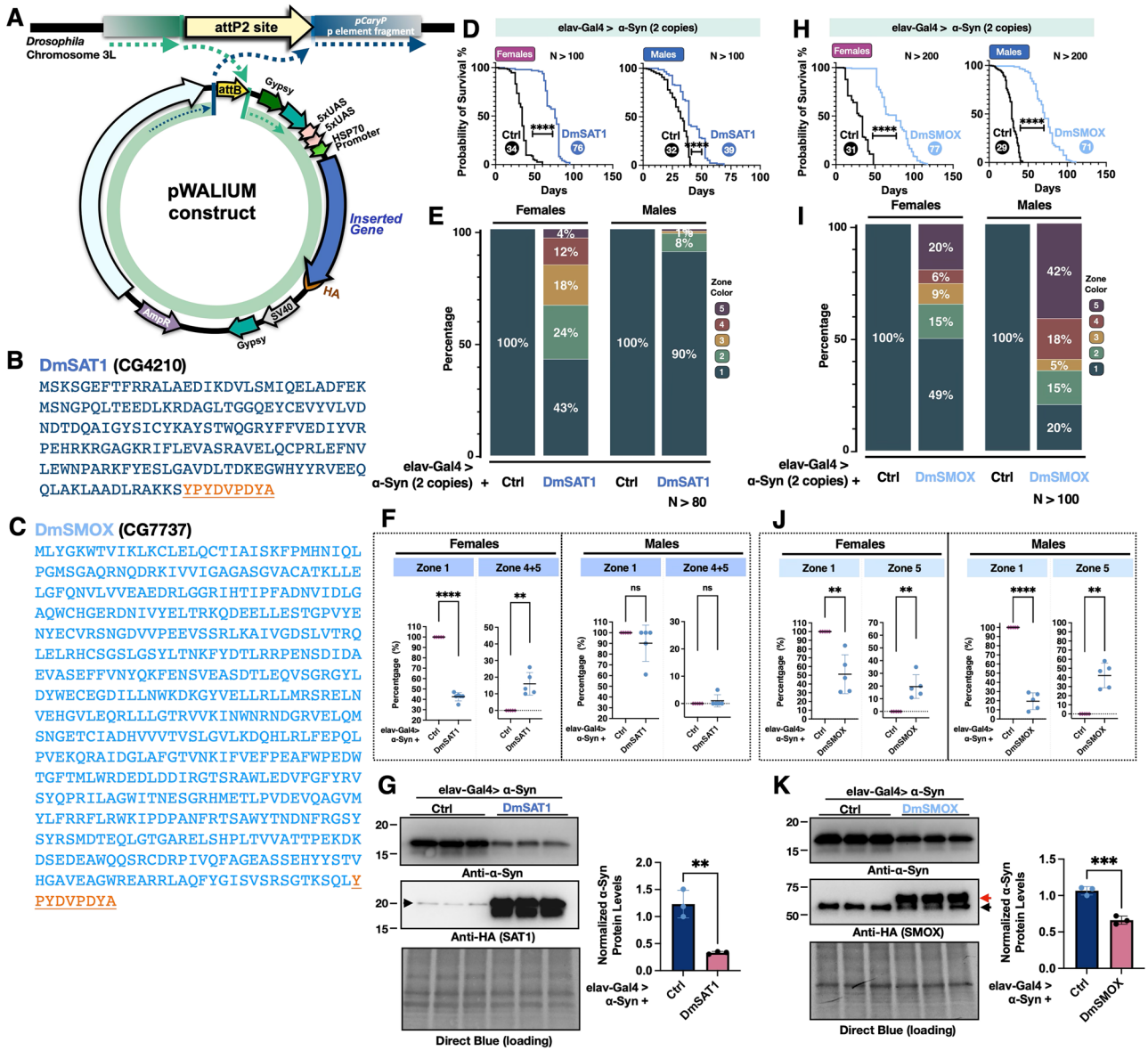

Fig. 6 | Overexpression of DmSAT1 and DmSMOX alters disease-related phenotypes in the α-Syn *Drosophila* model. A A diagram of the cloning strategy used to insert DmSAT1 or DmSMOX into the pWALIUM10.moe vector, with plasmids integrated into the third chromosome of the pCary fly line at the attP2 site; **B**, **C** amino acid sequences of HA-tagged DmSAT1 (**B**) and DmSMOX (**C**), with the HA tag underlined in orange; **D**, **H** longevity analysis of flies with pan-neuronal expression of two copies of α-Syn, with or without overexpression of DmSAT1 (**D**) or DmSMOX (**H**), where the numbers in the circles indicate median survival days and statistical significance was determined using log-rank tests (ns: not significant, $*p < 0.05$, $**p < 0.01$, $***p < 0.001$, $****p < 0.0001$); **E**, **I** motility analysis using the RING assay at week 4 in flies expressing two copies of α-Syn, with or without DmSAT1 (**E**) or DmSMOX (**I**) overexpression. Zone-specific comparisons from each RING assay (**E**, **I**) are shown in (**F**, **J**). The percentages of flies in zone 1 (the bottom zone) and zones 4 + 5 (**F**) or 5 only (**J**) (the top zone) were calculated per vial, with each group consisting of 5 vials containing 20 flies each. Statistical analysis was performed using an unpaired two-tailed Welch's *t* test. Significance levels: ns (not significant), $*(p < 0.05)$, $**(p < 0.01)$, $***(p < 0.001)$, $****(p < 0.0001)$, using GraphPad Prism. **G**, **K** western blot analyses of α-Syn protein levels in flies with pan-neuronal expression of α-Syn, with or without DmSAT1 (**G**) or DmSMOX (**K**) overexpression, where the arrowhead in (**G**) indicates non-specific bands; and in (**K**), the red arrow marks SMOX-specific bands and the black arrow denotes non-specific bands. Statistical analysis for western blots was performed using an unpaired two-tailed Student's *t* test with significance levels as follows: ns (not significant), $*(p < 0.05)$, $**(p < 0.01)$, $***(p < 0.001)$, $****(p < 0.0001)$.

While females generally outlived males in our model, the effects of individual PAIE knockdowns were directionally consistent between sexes, with one notable exception. In the case of SAT1 knockdown, females displayed reduction in lifespan compared to controls, whereas males showed no significant change. This divergence suggests that SAT1 exert sex-specific effects on neuronal survival. One possibility is that males and females differ in their basal SAT1 expression or protein turnover rates, making females more susceptible to SAT1 loss. Importantly, SAT1 knockdown has broad cellular effects beyond PA catabolism, including modulation of stress response genes[94,95], chromatin remodeling[96,97], autophagy pathways[95], hypoxia signaling (via HIF-1α)[94,98], and mRNA translation (via eIF5A hypusination)[99–101]. These downstream processes may also differ between sexes, amplifying the phenotypic disparity. Future studies are needed to dissect the sex-specific roles of SAT1 and to identify the molecular mechanisms driving these differential responses.

We also observed that SMOX overexpression improved climbing ability in both sexes, with a more pronounced effect in males (Fig. 6I). A greater proportion of male flies reached the upper zones (zones 4 and 5) compared to females, indicating a sex-specific enhancement in motor

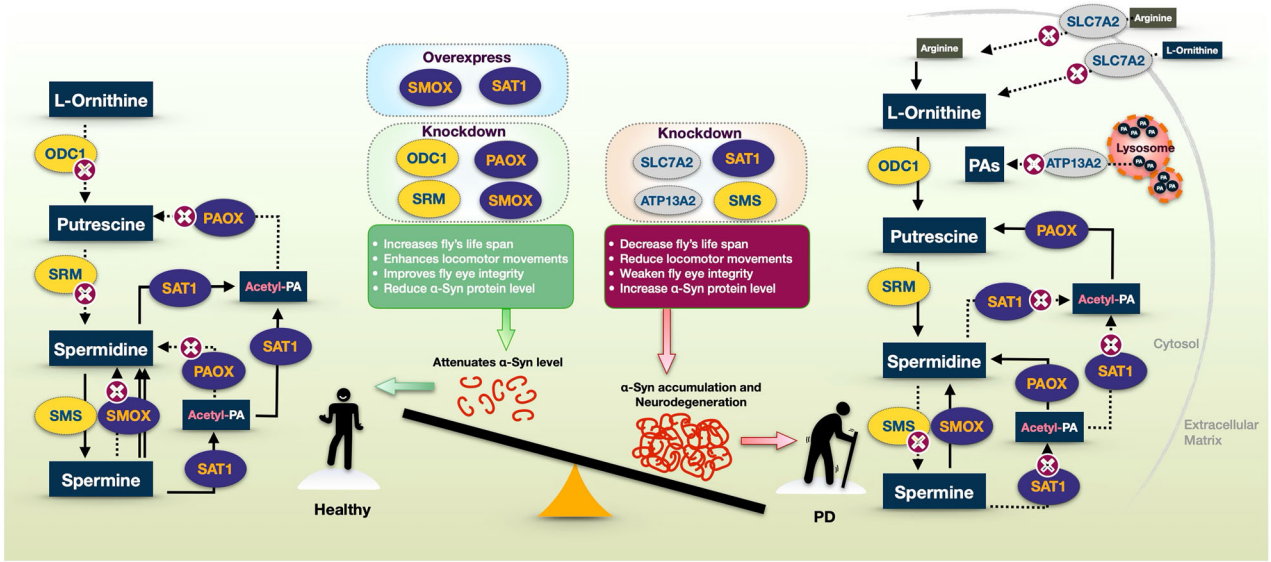

Fig. 7 | Proposed model of the polyamine pathway and its regulation of α-Synuclein levels and toxicity. Illustration of the PA pathway, emphasizing how the regulation of PAIE through RNAi knockdown (indicated magenta X-circles in the flow diagrams) or overexpression affects α-Syn protein levels and toxicity. The model highlights the influence of individual enzymes on polyamine metabolism, α-Syn accumulation, fly lifespan, motility, and eye integrity. The left half represents beneficial polyamine metabolism, where knockdown of ODC1, SRM, SMOX, or PAOX, or overexpression of SMOX or SAT1, reduces α-Syn levels and toxicity, promoting health and longevity. In contrast, the right half illustrates a PD-like condition, where knockdown of SMS, SAT1, ATP13A2, or SLC7A2 leads to either α-Syn accumulation or increased toxicity, ultimately resulting in neurodegeneration.

performance. Although the endogenous *SMOX* gene (CG7737) is located on the X chromosome, the overexpression construct used in our study was inserted into chromosome 3, thus avoiding direct effects of X-linked dosage compensation[102]. However, sex differences in the response to SMOX overexpression may still arise from underlying physiological or molecular differences between males and females[91,103]. For example, males may be more sensitive to changes in PA homeostasis or more responsive to elevated SMOX activity due to differential regulation of downstream targets, oxidative stress handling, or autophagic pathways. These findings suggest that sex is an important variable in determining the neuroprotective capacity of SMOX and should be considered in future studies aiming to dissect the mechanistic basis of PA-related interventions in α-Syn toxicity.

Our observation that both knockdown and overexpression of SMOX confer protective effects in the α-Syn *Drosophila* model was unexpected and suggests that SMOX may modulate α-Syn toxicity through multiple, potentially distinct mechanisms. SMOX catalyzes the oxidation of SPM to SPD, producing reactive oxygen species (ROS), including hydrogen peroxide (H_2O_2), as metabolic byproducts[61,104,105], which can contribute to oxidative stress. Partial suppression of SMOX may protect neurons by limiting ROS generation, thereby reducing oxidized α-Syn-induced toxicity and genomic damage[52]. This protective effect is supported by our western blot results showing reduced α-Syn protein accumulation, which correlates with improved cellular function as evidenced by extended lifespan, enhanced motility, and preserved neuronal integrity in the eyes. Subsequently, we observed that SMOX overexpression also produced a protective effect, which was unexpected given the benefits previously seen with SMOX knockdown. This intriguing result led us to further test whether overexpressing two copies of SMOX would yield an enhanced effect. As shown in supplementary fig. 3. Flies expressing two copies of DmSMOX exhibited a greater extension in median lifespan compared to those with non or only one copy (supplementary fig. 3A, B), with statistical significance observed in females based on the Gehan-Breslow-Wilcoxon test. In addition, Western blot analysis confirmed that two-copy DmSMOX overexpression reduces α-Syn protein level (supplementary fig. 3C). These results strengthen the evidence that SMOX overexpression confers neuroprotective effects and suggest that the degree of SMOX activity may differentially influence α-Syn pathology. Future work is needed to investigate how varying SMOX expression levels affect α-Syn aggregation, degradation, and associated neurotoxicity.

Mechanistically, SMOX catalyzes the conversion of SPM to SPD, a process that may facilitate the clearance of excess SPM and restore PA balance. In addition, elevated SPD levels have been associated with various beneficial effects, including stimulation of eIF5A hypusination[86,87], reduction of histone acetylation[106,107], and promotion of compensatory autophagy[108–110] and cellular repair processes[111]. These molecular changes may contribute to enhanced autophagic flux, supporting the removal of α-Syn aggregates and improving phenotypic outcomes[50]. This dual observation suggests that both reduced and elevated SMOX activity play a role in α-Syn toxicity, likely through different mechanisms.

Additionally, we found that neuronal knockdown of the PA transporters ATP13A2 and SLC7A2, as well as the catabolic enzyme PAOX, caused severe developmental abnormalities and led to early mortality in flies. These findings suggest that ATP13A2, SLC7A2, and PAOX are essential for normal developmental processes, potentially functioning both within and beyond their roles in maintaining PA homeostasis during development. Similarly, SAT1 knockdown was associated with increased α-Syn–related toxicity. As a rate-limiting enzyme in PA catabolism[62,112], SAT1 facilitates the acetylation of SPD and SPM, allowing these PAs to be further metabolized, reintegrated into other pathways, or exported from the cell. Reduced SAT1 activity may disrupt PA flux, resulting in the accumulation of SPD and SPM, which can become cytotoxic at elevated concentrations and compromise cellular homeostasis. In addition to its enzymatic role, SAT1 also interacts with other proteins and contributes to broader cellular functions[95,113]. For example, SAT1 has been shown to bind HIF-1α and RACK1, promoting the ubiquitination and degradation of HIF-1α[114], a transcription factor that regulates the expression of many stress- and metabolism-related genes[115,116]. Furthermore, the acetylation of PAs or other cellular targets may exert protective effects under conditions of cellular stress[59,117]. Taken together, our results suggest that SAT1 activity influences longevity, motility, and neuronal integrity in the α-Syn *Drosophila* model. The opposing outcomes observed with SAT1

knockdown versus overexpression indicate that SAT1 plays a protective role in α-Syn-induced toxicity, likely through both PA-dependent and independent mechanisms.

The PA pathway is highly interconnected and tightly regulated, making it challenging to consistently and persistently isolate the effects of a single enzyme. Modulating one PAIE can alter PA levels, which may in turn trigger compensatory responses from other enzymes within the same or related pathways to maintain cellular homeostasis. This dynamic balance reflects the regulatory mechanisms that cells employ to preserve homeostasis. The finding that both SMOX knockdown and overexpression confer protection from α-Syn likely reflects such compensatory dynamics. Overexpression of SMOX promotes the oxidation of SPM to SPD, generating hydrogen peroxide as a byproduct. In response to reduced SPM and elevated SPD levels, cells may activate additional regulatory mechanisms, including the modulation of PAIEs such as SAT1, SMS, SRM, and even SMOX itself, to restore PA balance. To address these complex interactions, future studies will need to incorporate metabolomic profiling, single-cell protein analysis, and single-cell RNA sequencing to monitor compensatory responses and clarify the specific roles of individual PAIEs at cellular resolution. Although disentangling these mechanisms is inherently challenging, we believe our findings represent a critical first step toward understanding how PA metabolism contributes to PD pathology.

Overall, our study demonstrates that specific PAIEs and PA transporters significantly affect the phenotypic outcomes of α-Syn-induced toxicity in a *Drosophila* model of PD. These findings highlight the importance of PA pathway regulation in modulating α-Syn homeostasis, neuronal integrity, and disease progression (Fig. 7). Future research should focus on dissecting the underlying molecular mechanisms and evaluating whether modulation of PAIE activity can serve as a viable therapeutic strategy. Moreover, given their strong influence on disease-relevant phenotypes, PAs, PAIEs, and related transporters may also hold promise as biomarkers[118,119] for early diagnosis and monitoring of PD[33]. Together, these insights position the PA pathway as a compelling target for both therapeutic intervention and biomarker development in synucleinopathies.

Methods

Drosophila stocks and maintenance

Stock numbers and genotypes of all flies are listed in Table 1. Publicly available stocks were obtained from the Bloomington *Drosophila* Stock Center (BDSC) or the Vienna *Drosophila* Resource Center (VDRC). Flies overexpressing UAS-DmSAT1 and UAS-DmSMOX were generated in our laboratory. cDNA of DmSAT1 (CG4210) and DmSMOX (CG7737) with an in-line HA tag was synthesized by GenScript (Piscataway, NJ), cloned into the pWalium10.moe plasmid, and injected into fly embryos for insertion into the attP2 site. Genomic DNA was extracted and sequenced to confirm line integrity and identity. Flies were reared in 5 mL of standard cornmeal fly medium supplemented with 2% agar, 10% sucrose, 10% yeast, and appropriate preservatives, under a 25°C incubator at 40% humidity with a 12/12-hour light/dark cycle. In all experiments, food vials were replaced every two to three days.

Longevity assay

Approximately 20 adult flies, matched by age and separated by sex within 48 hours of eclosion as adults from their pupal cases, were collected per vial and maintained on standard cornmeal fly medium at 25 °C. Flies were transferred to fresh food vials every 2–3 days, and mortality was monitored daily until all flies had died. Total fly numbers are indicated in each figure. Survival data were analyzed using the log-rank test in GraphPad Prism (San Diego, CA, USA).

Motility assay

Negative geotaxis was assessed through a modified RING assay[68,73,90] involving groups of at least 100 flies. Vials with 20 flies each were tapped to force them to settle at the bottom, and their climbing responses were captured with photographs taken 3 seconds afterward. Weekly records of the average performance from five consecutive trials were maintained. Between tests, flies were maintained on standard food. The positions of the flies within each vial were analyzed by dividing the vial into predefined zones. The number of flies in each zone was counted from the photographs and expressed as a percentage using RStudio (Boston, MA, USA), following the methodology described in our previous study[68].

CD8GFP fluorescence measurements

All flies analyzed in this study were heterozygous for both the driver (GMR-Gal4) and transgenes (UAS-CD8GFP and UAS-RNAi). Progeny were collected at eclosion and aged for 14 and 28 days. At these intervals, fly heads were dissected and imaged for GFP fluorescence using an Olympus BX53 microscope with a ×4 objective and a DP72 digital camera. The fluorescence intensity was quantified using ImageJ, as previously described[78,120]. Statistical analysis of GFP expression was performed using ANOVA in GraphPad Prism 9 (San Diego, CA, USA). All groups had $n \geq 15$ flies.

Western blots

Fourteen fly heads (seven males, seven females) per replicate were homogenized in hot lysis buffer (50 mM Tris pH 6.8, 2% SDS, 10% glycerol, 100 mM dithiothreitol), sonicated, boiled for 10 minutes, and centrifuged at maximum speed for 10 minutes. Protein lysates from at least three replicates were analyzed by western blotting using 4–20% Mini-PROTEAN® TGX™ Gels (Bio-Rad) and transferred to 0.2 µm PVDF membranes. After blocking in 5% milk/TBST, membranes were incubated overnight at 4 °C with primary antibodies: mouse anti-α-Syn (4B12, MA1-90346) (1:1000, ThermoFisher Scientific) and anti-HA (1:1000, Cell Signaling Technology), followed by secondary peroxidase-conjugated antibodies (1:5000, Jackson ImmunoResearch) for 1 hour at room temperature. Signal detection used EcoBright Pico/Femto HRP substrates (Innovative Solutions), imaged on a ChemiDoc system (Bio-Rad). PVDF membranes were stained with 0.1% Direct Blue 71 for total protein visualization[121–123]. The band intensities for α-Syn were quantified using ImageLab software (Bio-Rad). To normalize α-Syn levels, the intensity of the α-Syn band was divided by the total protein signal from Direct Blue 71 staining, which was measured across a standardized area of the full lane[122,124]. This approach ensures consistency across blots and accounts for variation in protein loading.

qRT-PCR

qRT-PCR was employed to quantify mRNA levels following PAIE knockdown (supplementary fig. 1). Total RNA was extracted from 14 fly heads per sample (six biological replicates per group) using TRIzol reagent (Invitrogen, Waltham, MA, USA) and treated with TURBO DNase (Invitrogen) to eliminate genomic DNA contamination. cDNA was synthesized using the High-Capacity cDNA Reverse Transcription Kit (Applied Biosystems, Waltham, MA, USA). Primer sequences are provided in supplementary fig. 1A. Quantitative PCR was performed on a StepOnePlus Real-Time PCR System (ThermoFisher Scientific) using Fast SYBR Green Master Mix (Applied Biosystems). Expression levels were normalized to the internal control gene rp49. Statistical analysis was conducted using an unpaired two-tailed Student's *t* test in GraphPad Prism (San Diego, CA, USA). Significance thresholds were defined as: ns (not significant), *($p < 0.05$), **($p < 0.01$), ***($p < 0.001$), ****($p < 0.0001$).

Statistics

All statistical analyses for longevity, motility assays, eye scoring, and Western blotting are described in the corresponding figure legends. For Western blot analyses, α-Syn levels were normalized to total protein as measured by Direct Blue 71 staining and compared to the appropriate control groups. Prism 9 (GraphPad) was used for data visualization and statistical analyses.

Table 1 | The genotype of files used in each figure

Gene	Fly gene identifier	Fly stock number	Genotype	Phenotype when expressed in neuron	Used in figures
PA anabolic enzymes					
UAS-ODC1$_{RNAi}$	CG8721	VDRC 30038	w1118; P{GD15056}v30038	Normal adults	Figs. 2–5
UAS-ODC1$_{RNAi}$	CG8721	VDRC 30039	w1118; P{GD15056}v30039/TM3	Normal adults	Data not included. An extra line for confirming the results.
UAS-SRM$_{RNAi}$	CG8327	VDRC 35883	w1118; P{GD13894}v35883	Normal adults	Figs. 2–5
UAS-SRM$_{RNAi}$	CG8327	BDSC 56011	y1 sc*v1 sev21; P{TRiP.HMC04307} attP40	Normal adults	Not in figures. An extra line for confirming the results.
UAS-SMS$_{RNAi}$	CG4300	VDRC 26500	w1118; P{GD11280}v26500	Normal adults	Figs. 2–5
UAS-SMS$_{RNAi}$	CG4300	BDSC 52924	y1 sc*v1 sev21; P{TRiP.HMC03665} attP40	Normal adults	Not in figures. An extra line for confirming the results.
PA catabolic enzymes					
UAS-SMOX$_{RNAi}$	CG7737	BDSC 36904	y1 sc*v1 sev21; P{TRiP.GL01104}attP2	Normal adults	Figs. 2–5
UAS-SMOX$_{RNAi}$	CG7737	VDRC 49437	w1118; P{GD9951}v49437	Normal adults	Not in figures. An extra line for confirming the results.
UAS-SAT1$_{RNAi}$	CG4210	VDRC 104004	w1118; P{KK107727}VIE-260B	Normal adults	Figs. 2–5
UAS-SAT1$_{RNAi}$	CG4210	BDSC 50615	y1 v1; P{TRiP.HMC02982}attP2/ TM3, Sb1	Normal adults	Not in figures. An extra line for confirming the results.
UAS-PAOX$_{RNAi}$	CG8032	VDRC 108652	w1118; P{KK100284}VIE-260B	Adults have developmental issues, such as unexpanded wings, and premature death.	Figs. 2–5
UAS-PAOX$_{RNAi}$	CG8032	BDSC 66967	y1 sc*v1 sev21; P{TRiP.HMS05433} attP40	Adults have developmental issues, such as unexpanded wings, and premature death.	Not in figures. An extra line for confirming the results.
PA transporters					
UAS-Anne (ATP13A2)$_{RNAi}$	CG32000	VDRC 105477	w1118; P{KK107621}VIE-260B	Adults have developmental issues, such as unexpanded wings, and premature death.	Figs. 2–5
UAS-Anne (ATP13A2)$_{RNAi}$	CG32000	VDRC 29174	w1118; P{GD14627}v29174/TM3	Adults have developmental issues, such as unexpanded wings, and premature death.	Not in figures. An extra line for confirming the results.
UAS-SLC7A2$_{RNAi}$	CG7255	VDRC 107802	w1118; P{KK110010}VIE-260B	Adults have developmental issues, such as unexpanded wings, and premature death.	Figs. 2–5
Others					
UAS-α-Syn	Human gene	BDSC 51374	w1118; P{w[+mC]=UAS-SNCA.J}4	Normal adults	Figs. 1–6
UAS-α-Syn	Human gene	BDSC 95240	w1118; P{w[+mC]=UAS-Hsap \SNCA.T}LP2	Normal adults	Not in figures. An extra line for confirming the results.
elav-Gal4	Gal4	BDSC 458	w1118; P{GawB}elav[C155]	Unable to apply	Figs. 1–3, 5, 6
sqh-Gal4	Gal4	Gift from Dr. Daniel Kiehart	w1118; sqh-Gal4; +	Unable to apply	Fig. 1
GMR-Gal4	Gal4	BDSC8605	w1118; +; GMR-Gal4	Unable to apply	Fig. 4
UAS-CD8GFP	Membrane-GFP	BDSC 5130	w1118; +;P{w+mC=UAS-mCD8::GFP.L}LL6	Normal adults	Fig. 4
UAS-Ctrl	-	Gift from Jamie Roebuck (Duke U)	y, w; +; attP2 landing site	Normal adults	Figs. 1 and 6
UAS-Ctrl$_{RNAi}$	-	VDRC 60000	w1118	Normal adults	Figs. 2–5

Data availability

Fly lines and source data are available upon request. The authors affirm that all data necessary for confirming the conclusions of the article are present within the article and figures. To request data from this study, please contact W-L. T at wtsou@wayne.edu.

Code availability

RStudio code (Boston, MA, USA) for converting fly counts of all zones into percentages and generating bar graphs is available upon request. Contact W-L. T at wtsou@wayne.edu to obtain the code from this study.

Received: 12 May 2025; Accepted: 19 July 2025;
Published online: 06 August 2025

References

1. Louis, E. D., Mayer, S. A. & Noble, J. M. *Merritt's neurology. Parkinson's disease by LeWitt PA*, (Wolters Kluwer, New York, 2021).
2. Morris, H. R., Spillantini, M. G., Sue, C. M. & Williams-Gray, C. H. The pathogenesis of Parkinson's disease. *Lancet* **403**, 293–304 (2024).
3. Deliz, J. R., Tanner, C. M. & Gonzalez-Latapi, P. Epidemiology of Parkinson's disease: an update. *Curr. Neurol. Neurosci. Rep.* **24**, 163–179 (2024).
4. Klein, C. & Westenberger, A. Genetics of Parkinson's disease. *Cold Spring Harb. Perspect. Med.* **2**, a008888 (2012).
5. Westenberger, A., Bruggemann, N. & Klein, C. Genetics of Parkinson's disease: from causes to treatment. *Cold Spring Harb. Perspect. Med.* **15**, a041774 (2024).
6. LeWitt, P. A. & Jenner, P. Introduction. *Parkinsonism Relat. Disord.* **80**, S1–S2 (2020).
7. Brichta, L. & Greengard, P. Molecular determinants of selective dopaminergic vulnerability in Parkinson's disease: an update. *Front Neuroanat.* **8**, 152 (2014).
8. Sonne, J., Reddy, V. & Beato, M. R. Neuroanatomy, substantia nigra. In *StatPearls* (Treasure Island, FL, 2025).
9. Agim, Z. S. & Cannon, J. R. Dietary factors in the etiology of Parkinson's disease. *Biomed. Res Int* **2015**, 672838 (2015).
10. Sosero, Y. L. & Gan-Or, Z. LRRK2 and Parkinson's disease: from genetics to targeted therapy. *Ann. Clin. Transl. Neurol.* **10**, 850–864 (2023).
11. Menozzi, E., Toffoli, M. & Schapira, A. H. V. Targeting the GBA1 pathway to slow Parkinson disease: Insights into clinical aspects, pathogenic mechanisms and new therapeutic avenues. *Pharm. Ther.* **246**, 108419 (2023).
12. Flagmeier, P. et al. Mutations associated with familial Parkinson's disease alter the initiation and amplification steps of alpha-synuclein aggregation. *Proc. Natl. Acad. Sci. USA* **113**, 10328–10333 (2016).
13. Meade, R. M., Fairlie, D. P. & Mason, J. M. Alpha-synuclein structure and Parkinson's disease - lessons and emerging principles. *Mol. Neurodegener.* **14**, 29 (2019).
14. Kouli, A., Torsney, K. M. & Kuan, W. L. Parkinson's disease: etiology, neuropathology, and pathogenesis. In *Parkinson's Disease: Pathogenesis and Clinical Aspects* (eds. Stoker, T. B. & Greenland, J. C.) (Brisbane (AU), 2018).
15. Calabresi, P. et al. Alpha-synuclein in Parkinson's disease and other synucleinopathies: from overt neurodegeneration back to early synaptic dysfunction. *Cell Death Dis.* **14**, 176 (2023).
16. Burre, J. The synaptic function of alpha-synuclein. *J. Parkinsons Dis.* **5**, 699–713 (2015).
17. Sharma, M. & Burre, J. Alpha-synuclein in synaptic function and dysfunction. *Trends Neurosci.* **46**, 153–166 (2023).
18. Vidovic, M. & Rikalovic, M. G. Alpha-synuclein aggregation pathway in parkinson's disease: current status and novel therapeutic approaches. *Cells* **11**, 1732 (2022).
19. Power, J. H., Barnes, O. L. & Chegini, F. Lewy bodies and the mechanisms of neuronal cell death in Parkinson's disease and dementia with Lewy bodies. *Brain Pathol.* **27**, 3–12 (2017).
20. Hindle, J. V. Ageing, neurodegeneration and Parkinson's disease. *Age Ageing* **39**, 156–161 (2010).
21. Thorne, N. J. & Tumbarello, D. A. The relationship of alpha-synuclein to mitochondrial dynamics and quality control. *Front. Mol. Neurosci.* **15**, 947191 (2022).
22. Han, D., Zheng, W., Wang, X. & Chen, Z. Proteostasis of alpha-synuclein and its role in the pathogenesis of Parkinson's disease. *Front. Cell Neurosci.* **14**, 45 (2020).
23. Jiang, P., Gan, M., Yen, S. H., McLean, P. J. & Dickson, D. W. Impaired endo-lysosomal membrane integrity accelerates the seeding progression of alpha-synuclein aggregates. *Sci. Rep.* **7**, 7690 (2017).
24. Brakedal, B., Toker, L., Haugarvoll, K. & Tzoulis, C. A nationwide study of the incidence, prevalence and mortality of Parkinson's disease in the Norwegian population. *NPJ Parkinsons Dis.* **8**, 19 (2022).
25. Vishwanathan Padmaja, M., Jayaraman, M., Srinivasan, A. V., Srikumari Srisailapathy, C. R. & Ramesh, A. The SNCA (A53T, A30P, E46K) and LRRK2 (G2019S) mutations are rare cause of Parkinson's disease in South Indian patients. *Parkinsonism Relat. Disord.* **18**, 801–802 (2012).
26. Book, A. et al. A meta-analysis of alpha-synuclein multiplication in familial parkinsonism. *Front Neurol.* **9**, 1021 (2018).
27. Srinivasan, E. et al. Alpha-synuclein aggregation in Parkinson's disease. *Front. Med.***8**, 736978 (2021).
28. Konno, T., Ross, O. A., Puschmann, A., Dickson, D. W. & Wszolek, Z. K. Autosomal dominant Parkinson's disease caused by SNCA duplications. *Parkinsonism Relat. Disord.* **22**, S1–S6 (2016).
29. Fuchs, J. et al. Phenotypic variation in a large Swedish pedigree due to SNCA duplication and triplication. *Neurology* **68**, 916–922 (2007).
30. Ball, N., Teo, W. P., Chandra, S. & Chapman, J. Parkinson's disease and the environment. *Front. Neurol.* **10**, 218 (2019).
31. Ghosh, S. et al. alpha-synuclein aggregates induce c-Abl activation and dopaminergic neuronal loss by a feed-forward redox stress mechanism. *Prog. Neurobiol.* **202**, 102070 (2021).
32. Deas, E. et al. Alpha-synuclein oligomers interact with metal ions to induce oxidative stress and neuronal death in Parkinson's disease. *Antioxid. Redox Signal.* **24**, 376–391 (2016).
33. PA, L., L, H. & R, P. Polyamine biomarkers of Parkinson's disease progression. *Mov. Disord.* **37**, S16–S17 (2022).
34. LeWitt, P. A., Li, J., Wu, K. H. & Lu, M. Diagnostic metabolomic profiling of Parkinson's disease biospecimens. *Neurobiol. Dis.* **177**, 105962 (2023).
35. Miller-Fleming, L., Olin-Sandoval, V., Campbell, K. & Ralser, M. Remaining mysteries of molecular biology: the role of polyamines in the cell. *J. Mol. Biol.* **427**, 3389–3406 (2015).
36. Nitta, T., Igarashi, K. & Yamamoto, N. Polyamine depletion induces apoptosis through mitochondria-mediated pathway. *Exp. Cell Res.* **276**, 120–128 (2002).
37. Ruiz-Chica, J., Medina, M. A., Sanchez-Jimenez, F. & Ramirez, F. J. Fourier transform Raman study of the structural specificities on the interaction between DNA and biogenic polyamines. *Biophys. J.* **80**, 443–454 (2001).
38. Yamashita, T. et al. Role of polyamines at the G1/S boundary and G2/M phase of the cell cycle. *Int. J. Biochem. Cell Biol.* **45**, 1042–1050 (2013).
39. Isa, T., Iino, M., Itazawa, S. & Ozawa, S. Spermine mediates inward rectification of Ca(2+)-permeable AMPA receptor channels. *Neuroreport* **6**, 2045–2048 (1995).
40. Skatchkov, S. N. et al. Spatial distribution of spermine/spermidine content and K(+)-current rectification in frog retinal glial (Muller) cells. *Glia* **31**, 84–90 (2000).

41. Sanchez-Jimenez, F., Medina, M. A., Villalobos-Rueda, L. & Urdiales, J. L. Polyamines in mammalian pathophysiology. *Cell Mol. Life Sci.* **76**, 3987–4008 (2019).
42. Casero, R. A. Jr. et al. Cytotoxic response of the relatively difluoromethylornithine-resistant human lung tumor cell line NCI H157 to the polyamine analogue N1,N8-bis(ethyl)spermidine. *Cancer Res.* **47**, 3964–3967 (1987).
43. Pledgie, A. et al. Spermine oxidase SMO(PAOh1), Not N1-acetylpolyamine oxidase PAO, is the primary source of cytotoxic H2O2 in polyamine analogue-treated human breast cancer cell lines. *J. Biol. Chem.* **280**, 39843–39851 (2005).
44. Snezhkina, A. V. et al. The dysregulation of polyamine metabolism in colorectal cancer is associated with overexpression of c-Myc and C/EBPbeta rather than enterotoxigenic bacteroides fragilis infection. *Oxid. Med. Cell Longev.* **2016**, 2353560 (2016).
45. Soda, K. Polyamine intake, dietary pattern, and cardiovascular disease. *Med. Hypotheses* **75**, 299–301 (2010).
46. Cason, A. L. et al. X-linked spermine synthase gene (SMS) defect: the first polyamine deficiency syndrome. *Eur. J. Hum. Genet.* **11**, 937–944 (2003).
47. Bupp, C. et al. Bachmann-Bupp Syndrome. *GeneReviews®* (Seattle, WA, 1993).
48. Akinyele, O. et al. Impaired polyamine metabolism causes behavioral and neuroanatomical defects in a novel mouse model of Snyder-Robinson syndrome. *Dis. Model. Mech.* **17**, dmm050639 (2024).
49. Berezov, T. T. et al. A role of polyamine metabolism in the functional activity of the normal and pathological brain. *Zh. Nevrol.Psikhiatr. Im S S Korsakova* **113**, 65–70 (2013).
50. Buttner, S. et al. Spermidine protects against alpha-synuclein neurotoxicity. *Cell Cycle* **13**, 3903–3908 (2014).
51. Liu, J. H. et al. Acrolein is involved in ischemic stroke-induced neurotoxicity through spermidine/spermine-N1-acetyltransferase activation. *Exp. Neurol.* **323**, 113066 (2020).
52. Uemura, T. et al. Decrease in acrolein toxicity based on the decline of polyamine oxidases. *Int. J. Biochem Cell Biol.* **79**, 151–157 (2016).
53. Sparapani, M., Dall'Olio, R., Gandolfi, O., Ciani, E. & Contestabile, A. Neurotoxicity of polyamines and pharmacological neuroprotection in cultures of rat cerebellar granule cells. *Exp. Neurol.* **148**, 157–166 (1997).
54. Vrijsen, S., Houdou, M., Cascalho, A., Eggermont, J. & Vangheluwe, P. Polyamines in Parkinson's disease: balancing between neurotoxicity and neuroprotection. *Annu Rev. Biochem* **92**, 435–464 (2023).
55. Antony, T. et al. Cellular polyamines promote the aggregation of alpha-synuclein. *J. Biol. Chem.* **278**, 3235–3240 (2003).
56. Lewandowski, N. M. et al. Polyamine pathway contributes to the pathogenesis of Parkinson disease. *Proc. Natl. Acad. Sci. USA* **107**, 16970–16975 (2010).
57. Handa, A. K., Fatima, T. & Mattoo, A. K. Polyamines: bio-molecules with diverse functions in plant and human health and disease. *Front Chem.* **6**, 10 (2018).
58. Pegg, A. E. Mammalian polyamine metabolism and function. *IUBMB Life* **61**, 880–894 (2009).
59. Rhee, H. J., Kim, E. J. & Lee, J. K. Physiological polyamines: simple primordial stress molecules. *J. Cell Mol. Med.* **11**, 685–703 (2007).
60. Agostinelli, E. et al. Polyamines: fundamental characters in chemistry and biology. *Amino Acids* **38**, 393–403 (2010).
61. Murray Stewart, T., Dunston, T. T., Woster, P. M. & Casero, R. A. Jr Polyamine catabolism and oxidative damage. *J. Biol. Chem.* **293**, 18736–18745 (2018).
62. Casero, R. A. & Pegg, A. E. Polyamine catabolism and disease. *Biochem. J.* **421**, 323–338 (2009).
63. Kramer, D. L. et al. Polyamine acetylation modulates polyamine metabolic flux, a prelude to broader metabolic consequences. *J. Biol. Chem.* **283**, 4241–4251 (2008).
64. Sharpe, J. G. & Seidel, E. R. Polyamines are absorbed through a y+ amino acid carrier in rat intestinal epithelial cells. *Amino Acids* **29**, 245–253 (2005).
65. Sekhar, V., Andl, T. & Phanstiel, O. T. ATP13A3 facilitates polyamine transport in human pancreatic cancer cells. *Sci. Rep.* **12**, 4045 (2022).
66. LeWitt, P. A. et al. Linking biomarkers and pathways: investigating Polyamines' influence on a-synuclein in Parkinson's disease. *Mov. Disord.* **38**, S11–S12 (2023).
67. Tsou, W. L. et al. Polyamine pathways: a promising frontier for biomarkers and therapeutic targets in Parkinson's disease (PD). *Mov. Disord.* **39**, S426–S426 (2024).
68. Ranxhi, B. et al. The effect of AKT inhibition in alpha-synuclein-dependent neurodegeneration. *Front. Mol. Neurosci.* **18**, 1524044 (2025).
69. Rosado-Ramos, R. et al. Genipin prevents alpha-synuclein aggregation and toxicity by affecting endocytosis, metabolism and lipid storage. *Nat. Commun.* **14**, 1918 (2023).
70. Karess, R. E. et al. The regulatory light chain of nonmuscle myosin is encoded by spaghetti-squash, a gene required for cytokinesis in Drosophila. *Cell* **65**, 1177–1189 (1991).
71. Kiehart, D. P. et al. Drosophila crinkled, mutations of which disrupt morphogenesis and cause lethality, encodes fly myosin VIIA. *Genetics* **168**, 1337–1352 (2004).
72. Johnson, S. L. et al. Differential toxicity of ataxin-3 isoforms in Drosophila models of Spinocerebellar Ataxia Type 3. *Neurobiol. Dis.* **132**, 104535 (2019).
73. Gargano, J. W., Martin, I., Bhandari, P. & Grotewiel, M. S. Rapid iterative negative geotaxis (RING): a new method for assessing age-related locomotor decline in Drosophila. *Exp. Gerontol.* **40**, 386–395 (2005).
74. Marras, C. et al. Prevalence of Parkinson's disease across North America. *NPJ Parkinsons Dis.* **4**, 21 (2018).
75. Patel, R. & Kompoliti, K. Sex and gender differences in Parkinson's Disease. *Neurol. Clin.* **41**, 371–379 (2023).
76. Tsou, W. L. et al. DnaJ-1 and karyopherin alpha3 suppress degeneration in a new Drosophila model of Spinocerebellar Ataxia Type 6. *Hum. Mol. Genet.* **24**, 4385–4396 (2015).
77. Prifti, M. V. et al. Insights into dentatorubral-pallidoluysian atrophy from a new Drosophila model of disease. *Neurobiol. Dis.* **207**, 106834 (2025).
78. Burr, A. A., Tsou, W. L., Ristic, G. & Todi, S. V. Using membrane-targeted green fluorescent protein to monitor neurotoxic protein-dependent degeneration of Drosophila eyes. *J. Neurosci. Res.* **92**, 1100–1109 (2014).
79. Ashraf, N. S. et al. Druggable genome screen identifies new regulators of the abundance and toxicity of ATXN3, the Spinocerebellar Ataxia type 3 disease protein. *Neurobiol. Dis.* **137**, 104697 (2020).
80. Bae, D. H., Lane, D. J. R., Jansson, P. J. & Richardson, D. R. The old and new biochemistry of polyamines. *Biochim. Biophys. Acta Gen. Subj.* **1862**, 2053–2068 (2018).
81. Grabenauer, M. et al. Spermine binding to Parkinson's protein alpha-synuclein and its disease-related A30P and A53T mutants. *J. Phys. Chem. B* **112**, 11147–11154 (2008).
82. Cook, C., Stetler, C. & Petrucelli, L. Disruption of protein quality control in Parkinson's disease. *Cold Spring Harb. Perspect. Med* **2**, a009423 (2012).
83. Won, S. J. et al. Neuronal oxidative stress promotes alpha-synuclein aggregation in vivo. *Antioxidants***11**, 2466 (2022).

84. Feng, D. et al. Spermidine inactivates proteasome activity and enhances ferroptosis in prostate cancer. *Acta Pharm. Sin. B* **15**, 2095–2113 (2025).
85. Tao, X. et al. Phenylbutyrate modulates polyamine acetylase and ameliorates Snyder-Robinson syndrome in a Drosophila model and patient cells. *JCI Insight* **7**, e158457 (2022).
86. Zhang, H. et al. Polyamines control eIF5A hypusination, TFEB translation, and autophagy to reverse B cell senescence. *Mol. Cell* **76**, 110–125 e9 (2019).
87. Liang, Y. et al. eIF5A hypusination, boosted by dietary spermidine, protects from premature brain aging and mitochondrial dysfunction. *Cell Rep.* **35**, 108941 (2021).
88. Smeltzer, S. et al. Hypusination of Eif5a regulates cytoplasmic TDP-43 aggregation and accumulation in a stress-induced cellular model. *Biochim. Biophys. Acta Mol. Basis Dis.* **1867**, 165939 (2021).
89. Johnson, S. L., Tsou, W. L., Prifti, M. V., Harris, A. L. & Todi, S. V. A survey of protein interactions and posttranslational modifications that influence the polyglutamine diseases. *Front. Mol. Neurosci.* **15**, 974167 (2022).
90. Sujkowski, A. et al. Progressive degeneration in a new Drosophila model of spinocerebellar ataxia type 7. *Sci. Rep.* **14**, 14332 (2024).
91. Shingleton, A. W. & Vea, I. M. Sex-specific regulation of development, growth and metabolism. *Semin Cell Dev. Biol.* **138**, 117–127 (2023).
92. Smilowska, K. et al. The prevalence of Parkinson's disease in Poland: regional and sex-related differences. *J. Parkinsons Dis.* **14**, 521–532 (2024).
93. Hirsch, L., Jette, N., Frolkis, A., Steeves, T. & Pringsheim, T. The incidence of Parkinson's disease: a systematic review and meta-analysis. *Neuroepidemiology* **46**, 292–300 (2016).
94. Zheng, C. et al. A noncanonical role of SAT1 enables anchorage independence and peritoneal metastasis in ovarian cancer. *Nat. Commun.* **16**, 3174 (2025).
95. Ou, Y., Wang, S. J., Li, D., Chu, B. & Gu, W. Activation of SAT1 engages polyamine metabolism with p53-mediated ferroptotic responses. *Proc. Natl. Acad. Sci. USA* **113**, E6806–E6812 (2016).
96. Brett-Morris, A. et al. The polyamine catabolic enzyme SAT1 modulates tumorigenesis and radiation response in GBM. *Cancer Res.* **74**, 6925–6934 (2014).
97. Murthy, D. et al. Cancer-associated fibroblast-derived acetate promotes pancreatic cancer development by altering polyamine metabolism via the ACSS2-SP1-SAT1 axis. *Nat. Cell Biol.* **26**, 613–627 (2024).
98. Murthy, D. et al. The MUC1-HIF-1alpha signaling axis regulates pancreatic cancer pathogenesis through polyamine metabolism remodeling. *Proc. Natl. Acad. Sci. USA* **121**, e2315509121 (2024).
99. Mandal, S., Mandal, A., Johansson, H. E., Orjalo, A. V. & Park, M. H. Depletion of cellular polyamines, spermidine and spermine, causes a total arrest in translation and growth in mammalian cells. *Proc. Natl. Acad. Sci. USA* **110**, 2169–2174 (2013).
100. Puleston, D. J. et al. Polyamines and eIF5A hypusination modulate mitochondrial respiration and macrophage activation. *Cell Metab.* **30**, 352–363 e8 (2019).
101. Dever, T. E. & Ivanov, I. P. Roles of polyamines in translation. *J. Biol. Chem.* **293**, 18719–18729 (2018).
102. Larschan, E. et al. X chromosome dosage compensation via enhanced transcriptional elongation in Drosophila. *Nature* **471**, 115–118 (2011).
103. Georgiev, P., Chlamydas, S. & Akhtar, A. Drosophila dosage compensation: males are from Mars, females are from Venus. *Fly***5**, 147–154 (2011).
104. Vujcic, S., Diegelman, P., Bacchi, C. J., Kramer, D. L. & Porter, C. W. Identification and characterization of a novel flavin-containing spermine oxidase of mammalian cell origin. *Biochem J.* **367**, 665–675 (2002).
105. Wang, Y. et al. Cloning and characterization of a human polyamine oxidase that is inducible by polyamine analogue exposure. *Cancer Res.* **61**, 5370–5373 (2001).
106. Eisenberg, T. et al. Induction of autophagy by spermidine promotes longevity. *Nat. Cell Biol.* **11**, 1305–1314 (2009).
107. Pietrocola, F. et al. Spermidine induces autophagy by inhibiting the acetyltransferase EP300. *Cell Death Differ.* **22**, 509–516 (2015).
108. Hofer, S. J. et al. Mechanisms of spermidine-induced autophagy and geroprotection. *Nat. Aging* **2**, 1112–1129 (2022).
109. Madeo, F., Bauer, M. A., Carmona-Gutierrez, D. & Kroemer, G. Spermidine: a physiological autophagy inducer acting as an anti-aging vitamin in humans?. *Autophagy* **15**, 165–168 (2019).
110. Ren, J. & Zhang, Y. Targeting autophagy in aging and aging-related cardiovascular diseases. *Trends Pharm. Sci.* **39**, 1064–1076 (2018).
111. Minois, N., Carmona-Gutierrez, D. & Madeo, F. Polyamines in aging and disease. *Aging***3**, 716–732 (2011).
112. Yuan, F. et al. Spermidine/spermine N1-acetyltransferase-mediated polyamine catabolism regulates beige adipocyte biogenesis. *Metabolism* **85**, 298–304 (2018).
113. Thakur, V. S., Aguila, B., Brett-Morris, A., Creighton, C. J. & Welford, S. M. Spermidine/spermine N1-acetyltransferase 1 is a gene-specific transcriptional regulator that drives brain tumor aggressiveness. *Oncogene* **38**, 6794–6800 (2019).
114. Baek, J. H. et al. Spermidine/spermine N(1)-acetyltransferase-1 binds to hypoxia-inducible factor-1alpha (HIF-1alpha) and RACK1 and promotes ubiquitination and degradation of HIF-1alpha. *J. Biol. Chem.* **282**, 33358–33366 (2007).
115. Dengler, V. L., Galbraith, M. & Espinosa, J. M. Transcriptional regulation by hypoxia inducible factors. *Crit. Rev. Biochem. Mol. Biol.* **49**, 1–15 (2014).
116. Hwang, H. J. et al. Hypoxia inducible factors modulate mitochondrial oxygen consumption and transcriptional regulation of nuclear-encoded electron transport chain genes. *Biochemistry* **54**, 3739–3748 (2015).
117. Makhoba, X. H., Ragno, R., Kaiser, A. & Agostinelli, E. An undefined interaction between polyamines and heat shock proteins leads to cellular protection in plasmodium falciparum and proliferating cells in various organisms. *Molecules* **28**, 1686 (2023).
118. Schwarz, C. et al. Effects of spermidine supplementation on cognition and biomarkers in older adults with subjective cognitive decline: a randomized clinical trial. *JAMA Netw. Open* **5**, e2213875 (2022).
119. Jimenez Gutierrez, G. E. et al. The molecular role of polyamines in age-related diseases: an update. *Int. J. Mol. Sci.* **24**, 1646 (2023).
120. Tsou, W. L., Qiblawi, S. H., Hosking, R. R., Gomez, C. M. & Todi, S. V. Polyglutamine length-dependent toxicity from alpha1ACT in Drosophila models of spinocerebellar ataxia type 6. *Biol. Open* **5**, 1770–1775 (2016).
121. Aldridge, G. M., Podrebarac, D. M., Greenough, W. T. & Weiler, I. J. The use of total protein stains as loading controls: an alternative to high-abundance single-protein controls in semi-quantitative immunoblotting. *J. Neurosci. Methods* **172**, 250–254 (2008).
122. Zeng, L. et al. Direct Blue 71 staining as a destaining-free alternative loading control method for Western blotting. *Electrophoresis* **34**, 2234–2239 (2013).
123. Hong, H. Y., Yoo, G. S. & Choi, J. K. Direct Blue 71 staining of proteins bound to blotting membranes. *Electrophoresis* **21**, 841–845 (2000).
124. Gilda, J. E. & Gomes, A. V. Stain-Free total protein staining is a superior loading control to beta-actin for western blots. *Anal. Biochem.* **440**, 186–188 (2013).

Acknowledgements

This study was partially supported by the Sastry Foundation Endowed Chair in Neurology (P.A.L.), NIH grant R01NS086778 (S.V.T.), and the Thomas C.

Rumble University Graduate Fellowships Award (B.R.). We sincerely thank the Sastry Foundation for their generous support through the Sastry Foundation Endowed Parkinson's Disease Research Fund at Wayne State University School of Medicine. In memory of Dr. Sastry, we honor his enduring legacy and contributions to Parkinson's disease research.

Author contributions

B.R.: data curation, software, validation, formal analysis, writing and editing. Z.R.B.: data curation, validation, formal analysis, investigation, methodology. Z.M.C.: data curation, validation, formal analysis, investigation, methodology. Z.Q.: data curation, validation, formal analysis, investigation, methodology. N.N.I.: data curation, validation, formal analysis, investigation, methodology. S.V.T.: conceptualization, data curation, funding acquisition, software, formal analysis, validation, visualization, methodology, writing and editing. P.A.L.: conceptualization, funding acquisition, validation, investigation, visualization, methodology, writing and editing. W-L.T.: conceptualization, data curation, software, formal analysis, validation, investigation, visualization, methodology, writing and editing.

Competing interests

The authors declare no competing interests.

Additional information

Supplementary information The online version contains supplementary material available at https://doi.org/10.1038/s41531-025-01087-9.

Correspondence and requests for materials should be addressed to Peter A. LeWitt or Wei-Ling Tsou.

Reprints and permissions information is available at http://www.nature.com/reprints

Publisher's note Springer Nature remains neutral with regard to jurisdictional claims in published maps and institutional affiliations.

Open Access This article is licensed under a Creative Commons Attribution 4.0 International License, which permits use, sharing, adaptation, distribution and reproduction in any medium or format, as long as you give appropriate credit to the original author(s) and the source, provide a link to the Creative Commons licence, and indicate if changes were made. The images or other third party material in this article are included in the article's Creative Commons licence, unless indicated otherwise in a credit line to the material. If material is not included in the article's Creative Commons licence and your intended use is not permitted by statutory regulation or exceeds the permitted use, you will need to obtain permission directly from the copyright holder. To view a copy of this licence, visit http://creativecommons.org/licenses/by/4.0/.

© The Author(s) 2025